Doctoral School on Engineering Sciences
Università Politecnica delle Marche

Extended summary

Characterization of tubular anode-supported SOFCs generators

Curriculum: Energetica

Author

Emanuela Brunetti

Tutor

Fabio Polonara

Date: 30/01/2013

Abstract. Systems based on the technology of fuel cells are among the most promising for the production of electrical energy for their high energy efficiency, low environmental emissions and for the variety of applications. The technology is used for distributed generation, residential and industrial cogeneration and portable generation. Among the various types of fuel cells, the solid oxide fuel cells (SOFC) are having a growing interest because the high operating temperature makes this technology particularly attractive for micro-cogeneration. This thesis reports a theoretical and experimental work on a tubular anode-supported SOFC generator produced by Acumentrics Corporation. The activity was focused on the study of the thermal-fluid-dynamics and electrochemical reaction of a single tubular solid oxide fuel cell anode supported with the main objective of study the electrochemical reaction with ANSYS-FLUENT for the precise analysis of the phenomena involved in single cell. The same approach has been applied to the study of the of the stack and the cathode recuperator. All dimensional features and operational components considered were provided by Acumentrics Corporation.
Furthermore was carried out an experimental characterization of the performance a prototype SOFC generator, always provided by Acumentrics Corporation. The generator was installed in a test rig and it was powered by hydrogen. The data were interpreted through multivariate analysis. Through this analysis it was possible to derive general rules for describing the operation of the system and its response to the changes in the operational parameters even in conditions different from those experimented.

Keywords. SOFC, Tubular fuel cells, Power generation, Performance analysis.

1 Experimental characterization

1.1 Introduction

Solid oxide fuel cell (SOFC) power generation systems have been intensively developed and these machines are now nearly ready for commercialization. There are still few reports of field tests on these units [1-5], while in the last two decades researchers have been especially active in developing mathematical models [6-12] and the results of this research activity point to several issues open to further investigations:
- the heat, mass and charge transport in single cells and stacks still require in-depth study [13];
- only a few of published mathematical models have undergone experimental validation;
- the thermophysical properties and reaction kinetics of several materials at high temperatures are still not investigated [14-17].

The experimental activities conducted on SOFCs have been characterized mainly by: (i) the study of new materials [18]; (ii) developments in single cell design [19-21]; (iii) the development of cell manufacturing methods, with numerous studies on the parameters that influence the microstructure of the materials [20-23]. As a result, the open literature is still short of information on the validation of the generation system's performance as a whole.

The documented tests to date on SOFC generators focused on: a) durability under stressing; b) long-term life; c) performance. The tests conducted therefore focused mainly on durability. Concentrating now exclusively on the performance testing activities, a thorough description of experiments conducted on a SOFC generator is given in [19].

The SOFC generator's performance depends on the interactions between some of its sections. The constitutive elements of a SOFC generator are the balance of plant (BoP), the power conditioning system (PCS), the fuel cell stack, and the electronic control and monitoring system. In fact, the control of the electrochemical reaction in the stack gives rise to the optimal thermodynamic conditions for each electrical load required, but in this condition the PCS might operate at the point of minimum efficiency, reducing the electrical power generated. The control loops in the control system may also not always be set correctly when the unit operates under variable electrical loads [24], giving rise to further inefficiencies. The results of operating SOFC generators therefore still fall far short of the performance achievable with other more efficient power generation systems.

The performance characterization of the Gen521 is outlined below, based on data obtained from an experimental campaign processed using PCA. The data analysis also highlights how the machine's various operating parameters influence the performance in different working conditions. Finally, the data were used to develop simple but sufficiently accurate equations capable of defining the behavior of the Gen521.

Furthermore the activity was focused on the study of the thermo-fluid and electrochemical reaction of a single tubular anode-supported solid oxide fuel cell with the main objective of study the electrochemical reaction in ANSYS-FLUENT. The same approach has been applied to the study of the stack and the cathode recuperator. All dimensional features and operational components considered were provided by Acumentrics Corporation.

1.2 The test rig

An outdoor test rig was set up to quantify the performance of the Gen521 (Fig. 1) at the Dipartimento di Ingegneria Industriale e Scienze Matematiche of Universita` Politecnica delle Marche (Ancona, Italy). The test rig comprises a water demineralization unit where the water is treated before to enter in a electrolyzer. The electrolyzer produces hydrogen and oxygen separately. The hydrogen is collected and moved to a drying column and then to the SOFC generator. To charachterize the generator we set 5 switchable lights. Switching on 1 or more of these lights we can require more or less power production.

Figure 1 Test rig. 1. Demineralization unit 2. Demineralized water tank 3. Electrolyzer 4. Drying bed 5. Acumentrics Gen521 6. Lights 7. Exhaust duct

The Acumentrics generator presents 2 stacks. Each Stack has 12 rows. In each rows are collected 6 cells. The tubes in the stacks are 144 to produce 2.5kWel in a box of external dimensions: 86cmX145cmX127cm. The stacks are a part of the generator (Fig.2). In fact there are also the components to operate and regulate the unit (BoP) and the PCS. The PCS is the section dedicated to the conversion of the produced power (Fig. 3).

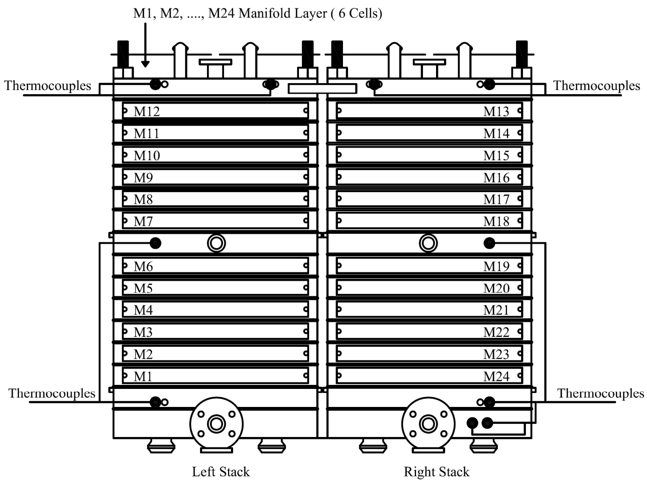

Figure 2 Map of measuring devices

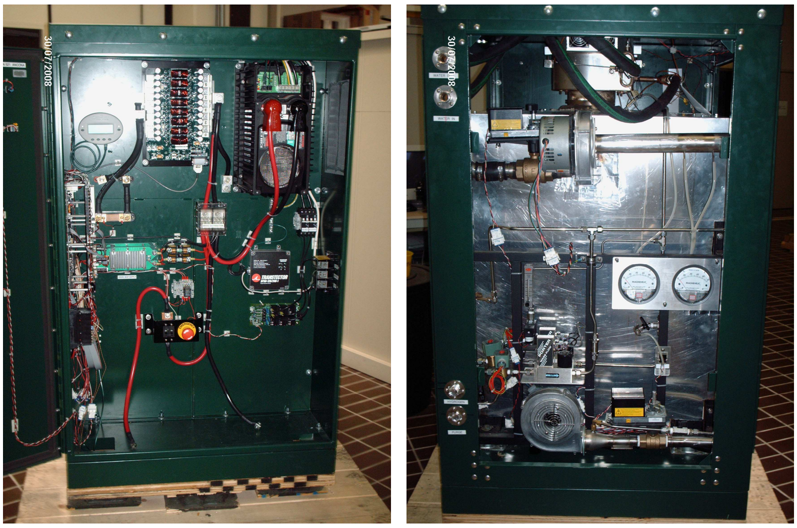

Figure 3 BoP end Pcs

1.3 Headings SOFC generator testing strategy

To conduct the tests some input and output variables were identified and the unit were treated as a black box where to see only the inputs and output changing. The interesting output was considered the stack voltage to follow the polarization curve of the unit at different working conditions. In particular, only the steady state working conditions were considered, so the tests consisted in changing some adjustable parameters and the electrical loads to 400W, 800W, 1000W, 1200Wand 1400W. The experimental data were obtained by combining the results recorded in these different operating conditions. The results were typically arrays of time-dependent values. This very large set of collected data was filtered using four criteria:

- stack temperatures: each temperature value acquired had to be no more than 2.5°C higher or lower than the mean temperature measured for the previous 600 s;
- the voltages measured for the 24 stacks: each voltage value acquired had to be no more than 0.01 V higher or lower than the mean voltage measured for the previous 600 s;
- battery voltage: each battery voltage value acquired had to be no more than 0.075 V higher or lower than the mean voltage measured for the previous 600 s;
- residence time of the value measured: all measured values had to satisfy the above conditions for at least 30 s.

The acquired data were reduced in number and were representative of genuinely stable operating conditions. The experimental data gave rise to numerous clusters, as shown in Fig. 4, so they were difficult to interpret and group into common working conditions. In fact observing the dependence of DC electrical power and SV on the current, in Fig. 4 might seem that there are three operating conditions.

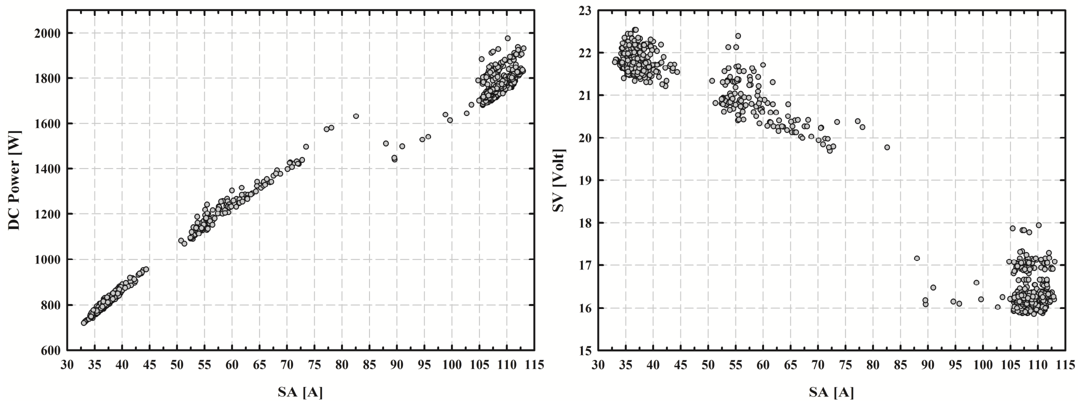

Figure 4 Experimental data collected for DC electrical power and SV in a steady state for different currents generated by the stacks

As emerges from the experimental data collected in Fig. 4, there was a higher density of acquisitions in certain current ranges because the tests were conducted at different electrical loads. Fig. 4 also shows a discontinuity in the DC electrical stack power at 85 A. This discontinuity highlights the different operating conditions imposed on the machine at the higher currents. Given this discontinuous trend of the DC stack power (DC power) and the stack voltage (SV), it became necessary to divide the operating domain between the higher currents (from 88.00 A to 112.8 A) and the lower currents (from 33.02 A to 82.57 A). These two zones into which the study was divided had the characteristics outlined in Table 1. Looking at the data in Table 1, the largest differences between the two datasets for the operating zones 1 and 2 clearly coincide with the global thermal gradient of the stacks (DT), the mean working temperature of the stacks (TM) and the utilization factor (FU). So our proposed characterization will therefore be divided into two parts depending on the stack current (SA) range.

Table 1. Description of the parameters and variables

Parameters	Units	I/O	Meaning	Zone 1		Zone 2	
				Min	Max	Min	Max
AirF	m3/s	In	Cathode air flow rate	0.00945	0.03183	0.01297	0.01550
HyF	m3/s	In	Anode hydrogen flow rate	0.00043	0.00059	0.00043	0.00047
HyP	Pa	In	Anode hydrogen pressure	101328	101807	101328	101807
RAirHy	--	In	Ratio between cathode and anode flows	21.11	55.57	28.96	33.86
SA	A	In	Current form the two stacks	33.02	82.57	88.00	112.80
TM	°C	In	Mean temperature in the stacks	767.20	811.15	739.30	758.70
DT	°C	In	Difference between maximum and minimum temperatures in the stacks	37.20	42.3	88.00	119.30
FU	%	In	Utilization factor	19.45	37.49	46.90	72.77
SV	V	Out	Stacks voltage	19.69	22.54	15.85	17.94

1.4 Analysis of the experimental data

Several clusters can be observed, which make it difficult to generalize the machine's operation. Some of the correlations in the machine's operation depend on the control system, which correlates certain variables that are themselves not correlated. In other cases, the parameters are correlated as a consequence of physical phenomena that influence each other. In other cases again, certain parameters are estimated starting from other parameters. DC Power and SV are considered machine output parameters. They are practically correlated with all the variables. We applied a Principal Component Analysis (PCA) on the experimental zones and a multi-linear regression. The data has been scaled because the units of measure of each parameter and variable differed. Conducting the analysis without completing this important preliminary step would produce errors because they would be influenced by the very different order of magnitude of the numerical values. Data scaling is therefore a step that enables the effects of different units of measure and variances on the PCA to be minimized. This scaling can be done in various ways. For the present problem, it was opted for a natural-logarithmic scaling of the data due to the large differences in the orders of magnitude between the numerical values and between their variances [25]. Then the PCA was conducted on the scaled data. PCA is mathematically defined as an orthogonal linear combination that transforms the data to a new coordinate system having the PCs as axes. PCA is a multivariate analysis of data method performed on a dataset for the purpose of identifying a limited number of parameters that account for most of the variance of the data. The method is therefore used to establish which parameters determine similarities between the data. In PCA the original set of parameters is converted into a new set comprising an equal number of independent uncorrelated principal components (PCs), which are linear combinations of the original parameters. Along the first coordinate (PC1) the greatest variance of data is present, then the second coordinate (PC2) adds another part of variance of data and so on for all PCs. At the end of the analysis, it is also obtained a sequential list of linear combinations that best explain the variance of the data and from these combinations it is possible to identify the parameters that affect the variance the most. From the viewpoint of the similarity of data instead of the variance, projecting the data onto a space that depends on the linear combination of the parameters enables us to identify any clusters, which represent similar operating conditions. The identification of different clusters leads to the determination of different operating conditions. Separately analyzing the data belonging to each cluster and the principal differences between the clusters, it can be identified which parameters influence the machine's performance.

1.5 Results

The above-described analysis enabled us to select a subset of parameters for modeling the unit's operating conditions. Fig. 4 shows a close correlation between SA and DC Power from which the correlation between SA and SV (the unit's polarization curve) could also be derived. Based on the previous PCA it could be developed a simplified equation in order to correlate SV and DC Power. Finally, two models needed to be developed, one for each zone investigated:

For SV in zone 1:

$$SV = 11.8130 - 336.752AirF - 190.904HyF + 9.602E\text{-}05HyP + 0.220732RAirHy - 0.71307Log(SA) + 0.00246678TM - 2.73473E\text{-}03DT - 0.0293085FU \quad \text{(eq 1)}$$

For SV in zone 2:

$$SV = -36.1716 - 1259.1AirF + 48582.8HyF - 8.602E\text{-}05HyP + 0.652632RAirHy + 0.266212Log(SA) + 0.0428924TM + 2.82523E\text{-}02DT + 0.00348682FU \quad \text{(eq 2)}$$

For DC Power in zone 1:

$$DC\ Power = -4074.78 - 5038.52AirF - 17626.0HyF + 9.491E\text{-}03HyP + 2.36355RAirHy + 924.802Log(SA) + 0.691061TM + 0.510723DT + 0.960723FU \quad \text{(eq 3)}$$

For DC Power in zone 2:

$$DC\ Power = -12912.3 - 188745.0AirF + 6968170HyF - 7.919E\text{-}03HyP + 74.2735RAirHy + 1710.24Log(SA) + 4.89874TM + 3.18359DT + 0.410075FU \quad \text{(eq 4)}$$

where Log is the natural logarithm.

If we plot the linear relations from the analysis we observe that using a full model comprising 6 variables we obtain R^2=0.98, while if we use a 2 variables (stack current and thermal gradient) model we obtain R^2=0.975. Regressing the data with the last model we could generalize the behavior of the unit. In fact we could plot the iso-gradient curves on the old graphs ad derive information about the limits of the unit (Fig. 5). The Fig. 6 shows the Eqs. (1)e(4) applied to a long operating period, also in unsteady states. Although large differences are evident during the start-up, these differences decrease in the transition period between two different steady states of the system. For DC Power the Eqs. (3) and (4) produce very similar values: this is because the parameters with the strongest influence on DC Power in zone 1 also influence zone 2.

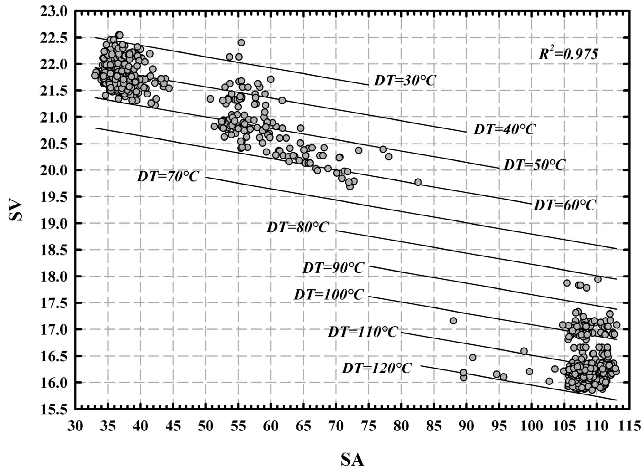

Figure 5 The polarization curves of the unit in the ohmic region

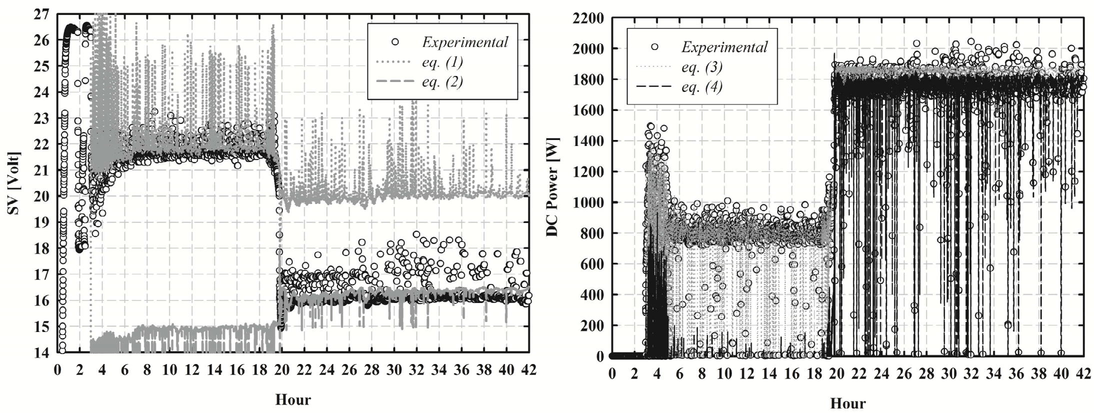

Figure 6 Stack voltage (left) and DC Power (right) during the transition between different steady states

1.6 Conclusions

Exclusively steady state conditions were investigated. It is difficult to deduce general rules from the data obtained because they consist of a considerable number of quantities that vary simultaneously, also on the basis of the inner control logic of the machine. The data collected were typically in the form of arrays of time-dependent values, so graphically representing the relationships between the working variables produced no evident trends, but clusters of points in certain operating regions, which represent different operating conditions. Performing a multivariate analysis on the data produced useful information for interpreting the system as a black box. The proposed data analysis enabled us to derive general rules that describe the system's operation, and to use said rules to study the system's response to variations in its operating parameters.

2 Thermo-fluid-dynamics study of a tubular solid oxide anode-supported fuel cell

The following part had the main objective of studying the electrochemical reaction with ANSYS-FLUENT for the precise analysis of the phenomena involved in single cell. The same approach has been applied to the study of the stack and the cathode recuperator. All dimensional features and operational components considered were provided by Acumentrics Corporation.

2.1 Description of the geometry and its relative discretization for the single cell

The geometrical model considered is represented in Fig. 7. The geometric model was discretized by meshing software present in the work platform ANSYS-WORKBENCH 12.1. Fig. 8 shows the discretized geometry in which the domain of the air has been hidden to display the cell tube.

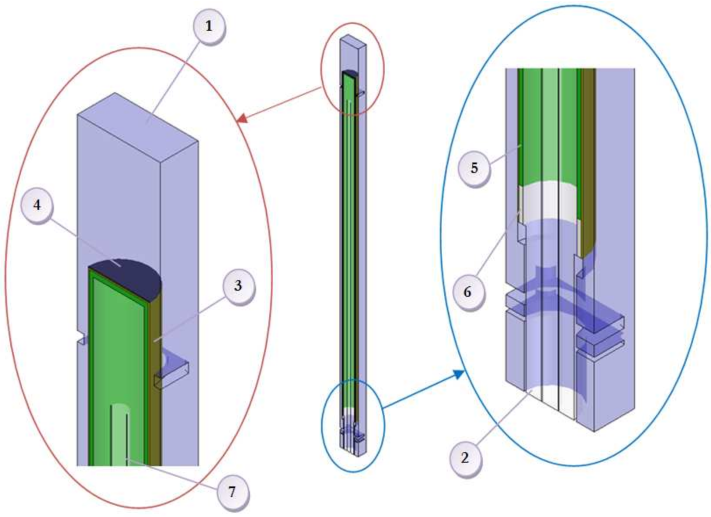

Figure 7 Overall view of the geometrical model. (3): cathode; (5): anode. The fuel cell is fed from a narrow hydrogen pipe (7) and surrounded on the outside by air (1), while the connections to the anode are represented by the volume (6) and those to the cathode by the volume (4)

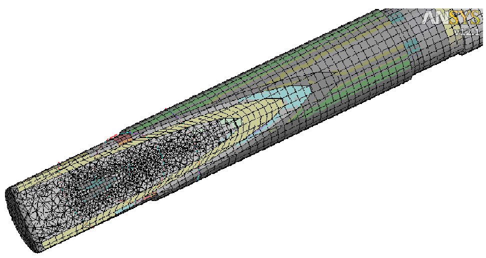

Figure 8 Discretized geometry

2.2 Description of the mathematical model and its implementation

The mathematical model is rather complex because, in addition to the thermo-fluid dynamic phenomena, there is also the electrochemical reaction. The model is based on the following assumptions: i) electrochemical reaction managed by unresolved electrolyte model; ii) air is an incompressible fluid; iii) steady state balances. The parameters used for the definition of the materials were taken in part in the literature among those more commonly used in the modeling studies of SOFC, and partly by Acumentrics. The boundary conditions at the inlet are defined in table 2

Table 2. Boundary condition inputs

	Value	Units
Anode Channel Flow		
Mass Flow Rate	1.8e-05	kg/s
Temperature	800	°C
Gas composition		
CO_2	1.4	% Vol
CO	17.6	% Vol
H_2	34.7	% Vol
H_2O	2.8	% Vol
N_2	43.5	% Vol
Cathode Channel Flow		
Mass Flow Rate	1.9e-04	kg/s
Temperature	675	°C
Gas composition		
O_2	21	% Vol
N_2	79	% Vol
Current take-off		
Anode	0	Volt
Cathode	0.65	Volt

2.3 Results

The Fig. 9 shows the most significant results obtained through simulation and objective of the study: the cell generates a potential difference of 0.65 volts to the take-offs generates a current of 46.9 amperes.

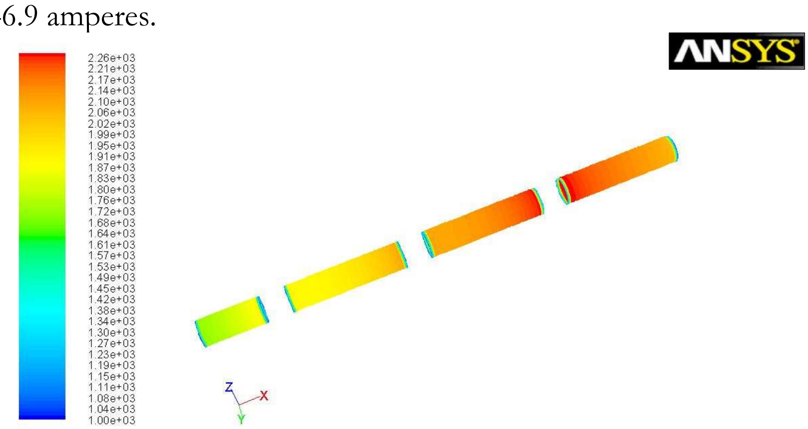

Figure 9 Current density in the following operational conditions: Average current density: 2039A/m²; Total current: 46.9A; Utilization factor: 49%

The part of the electrolyte next to the cathode current take-off has an increase of the current density because the electrochemical reaction is facilitated by the presence of more electrons. The current density presents a maximum. It is due to the uncorrect fuel/O_2 ratio near the end of the tube (Fig. 10).

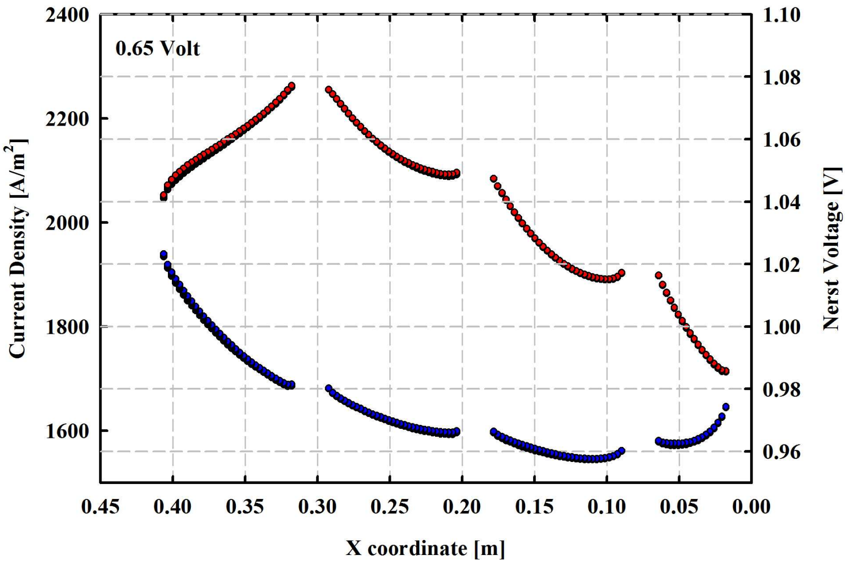

Figure 10 Trend of the current density and the reversible potential on the surface of the electrolyte

Changing from 0.5 Volts to 0.75 Volts, strong gradients appear in the electrolyte temperature field. (Fig. 11)

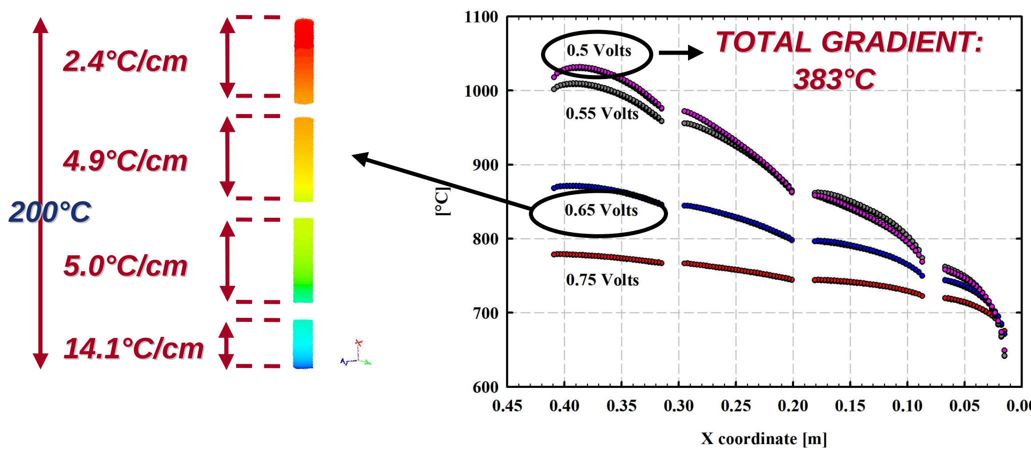

Figure 11 Electrolyte temperature fields

In the adduction tube is reached speed of 6.35 m/s at the maximum point and that is on the symmetry axis of the tube. When the fuel exits the pipe and enters the anode channel, the speed decreases greatly due to the greater section of the channel reaching maximum speeds of 0.5 m/s. The air externally reaches speeds of about 1.3 m/s.

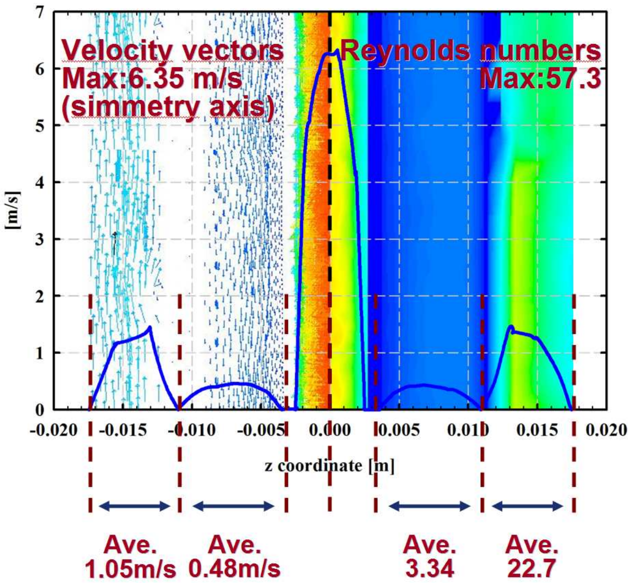

Figure 12 Velocity field

2.4 Description of the geometry and its relative discretization for the stack

The model was created on the basis of the geometry provided by Acumentrics. In the implementation of the geometrical model, we only considered the air volume with a single body. We considered only half of the geometry due to geometry symmetry. The Fig. 13 shows how this simplification was achieved and the discretized domain.

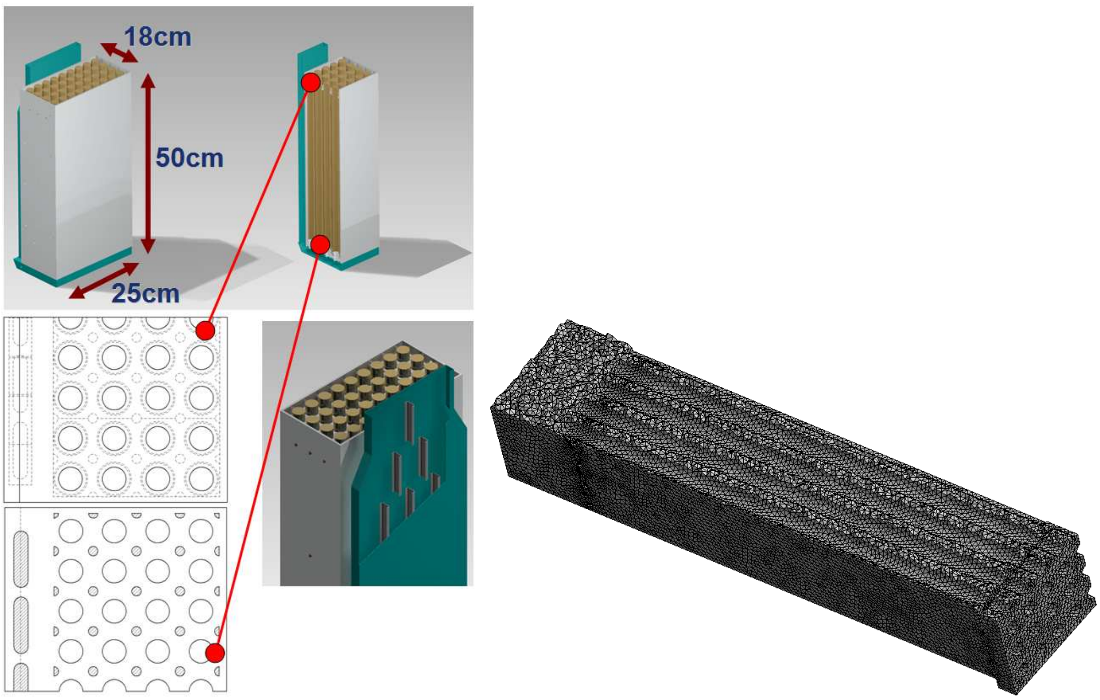

Figure 13 The stack (left side) and the discretized domain (right side)

2.5 Matematical model

The mathematical model describes the thermo-fluid-dynamic phenomena that occur within the stack and the downcomer on the air side. In this study, we did not consider the electrochemical reaction directly, instead we used a heat source term in the equation for the reaction energy into account. This model is based on the following and main assumptions: i) air is an ideal gas; ii) steady state balances; iii) k-ε RNG turbulence. The boundary conditions at the inlet were defined in table 3

Table 3. Boundary condition inputs

	Value	Units
Inlet Flow Rate	0.0069	kg/s
Inlet Pressure	450	Pa
Energy Source	22	W/m^2

2.6 Results

The streamlines are shown in Fig. 14. The main information are: (i) the maximum velocity: it is 27.6m/s at the bottom of the hot module (ii) the path followed by the flow: in the bundle zone the streamlines are collected centrally and the flow near the outer tubes is negligible.

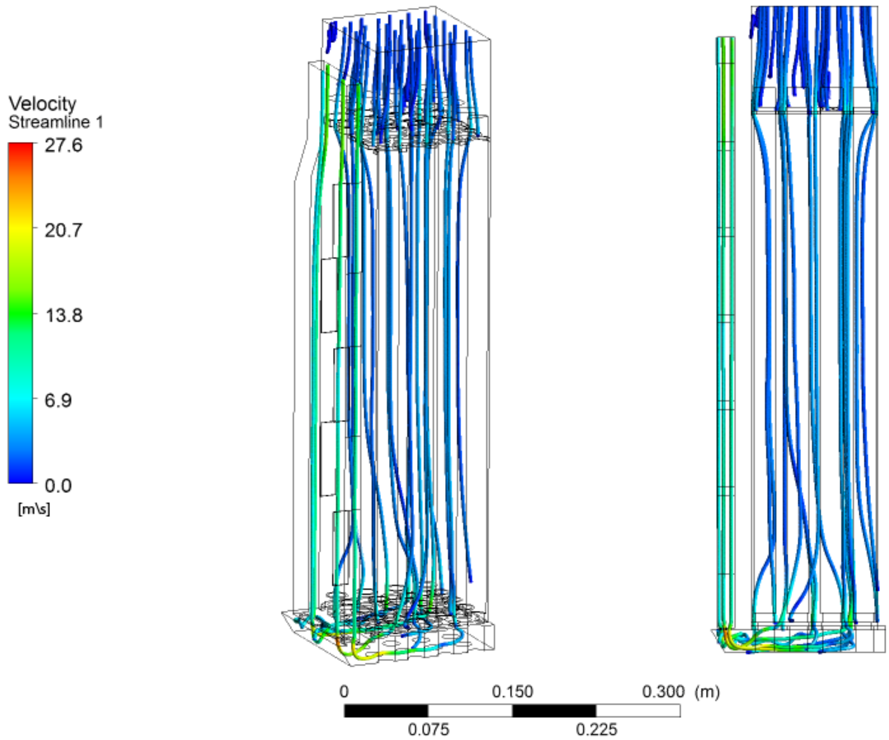

Figure 14 Pathlines

The Reynolds numbers confirm the presence of zones with low velocity of the air. Such zones are the peripheral zones. Moreover the bundle zone is characterized by a low velocity flow ranging between 2 and 13m/s (Fig. 15).

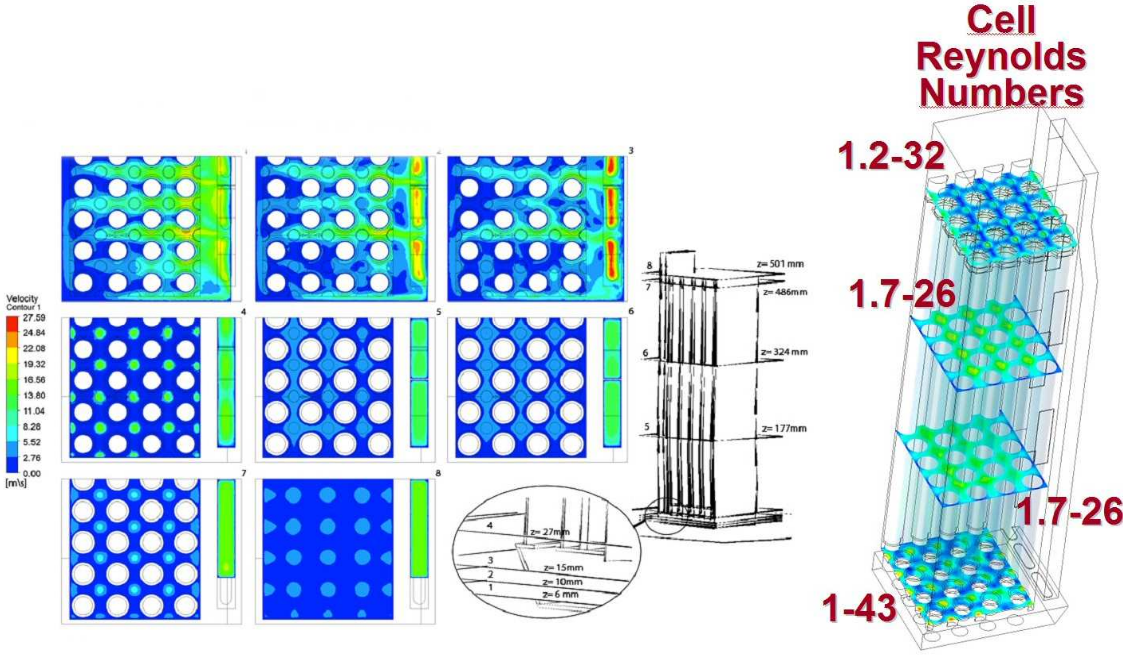

Figure 15 Velocity Field

The temperature field highlights the zones with stronger gradients. The tubes subjected to higher temperature gradients are the tubes more distant form the center (Fig. 16)

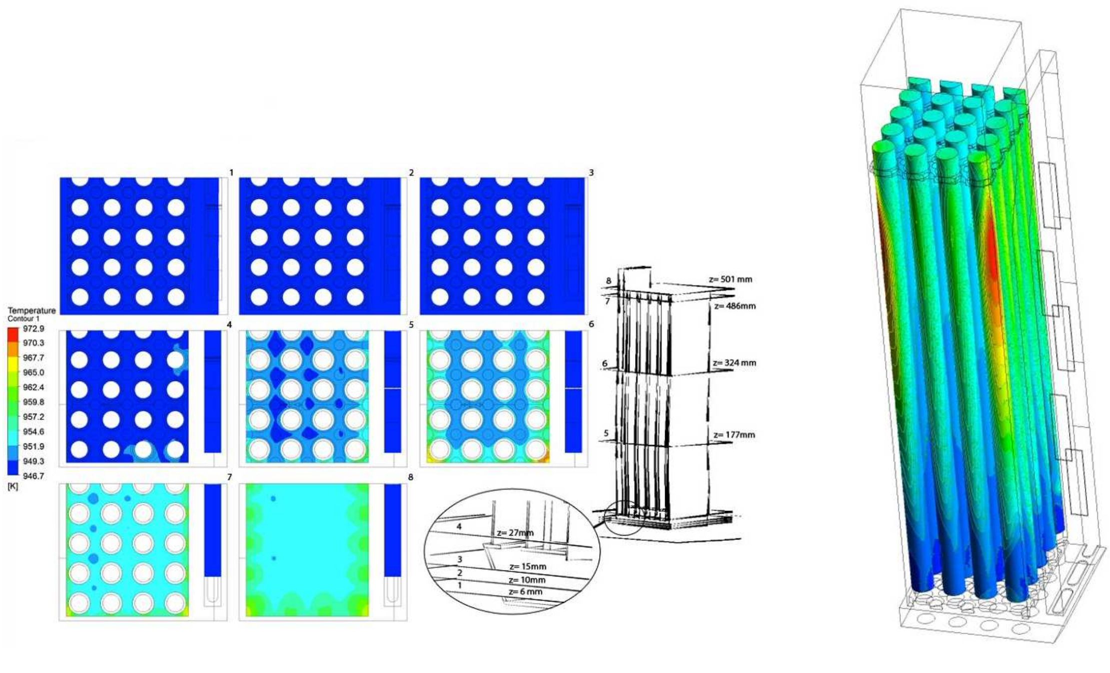

Figure 16 Temperature Field

Finally the maximum estimated heat transfer coefficient is 0.15W/m^{2}K with max Nusselt number of 5.9. That is due to the low turbulent intensity. In fact the zones where there are higher temperture gradients correspond to the zones where there are low heat transfer coefficients and probably natural convection (Fig. 17).

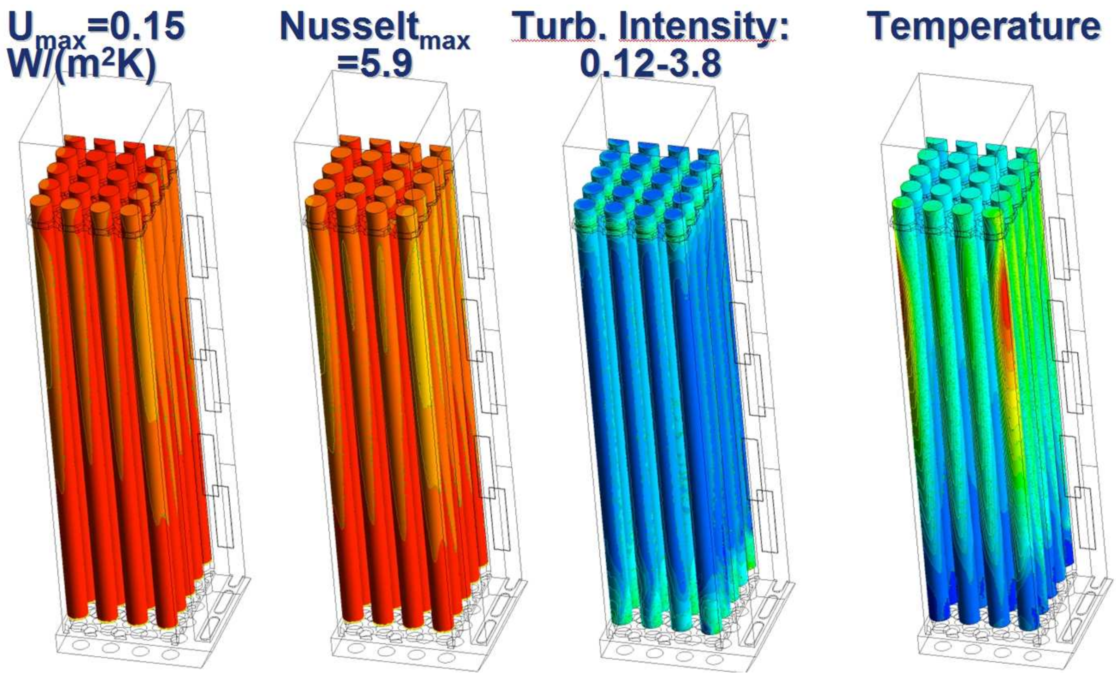

Figure 17 Estimated heat transfer coefficient

2.7 Conclusion

The chemical-thermal-CFD method can describe the operation of the device (hot module and single cell) and give a direction for further optimization. The optimization of the hot module and the single cell are still to be performed by Acumentrics on the basis of the presented results. In fact the bundle could operate in several zones in natural convection. For the single cell a deeper investigation on the reactor design is needed, oriented to the design improvements for performance maximization. In the future the study will be oriented for the integration between hot module and single cell models

References

[1] Munch W, Frey H, Edel M, Kessler A. Stationary fuel cells-Results of 2 years of operation at EnBW. J Power Sources 2006;155:77e82.

[2] Gariglio M, De Benedictis F, Santarelli M, Calı` M. Analysis of the cooling transient of a large SOFC generator. Int J Hydrogen Energy 2008;33:3204e8.

[3] Gariglio M, De Benedictis F, Santarelli M, Calı` M, Orsello G. Experimental activity on two tubular solid oxide fuel cell cogeneration plants in a real industrial environment. Int J Hydrogen Energy 2009;34:4661e8.

[4] Raymond AG. Status of tubular SOFC field unit demonstrations. J Power Sources 2000;86:134e9.

[5] Barrera R, De Biase S, Ginocchio S, Bedogni S, Montelatici L. Performance and life time test on a 5kW SOFC system for distributed cogeneration. Int J Hydrogen Energy 2008;33: 3193e6

[6] Bassette NF, Wepfer WJ, Winnick J. A mathematical model of a solid oxide fuel cell. J Electrochem Soc 1995;142(11): 3792e800.

[7] Chan SH, Khor KA, Xia ZT. A complete polarization model of a solid oxide fuel cell and its

sensitivity to the change of cell component thickness. J Power Sources 2001;93: 130e40.
[8] Gopalan S, Di Giuseppe G. A macro-level model for determining the performance characteristics of solid oxide fuel cells. J Power Sources 2004;125(2):183e8.
[9] Hernandez-Pacheco E, Singh D, Hutton PN, Patel N, Mann MD. A macro-level model for determining the performance characteristics of solid oxide fuel cells. J Power Sources 2004;138(1e2):174e86.
[10] Bharadwaj A, Archer DH, Rubin ES. Modeling the performance of a tubular solid oxide fuel cell. J Fuel Cell Sci Technol February 2005;2(1):1e7.
[11] Lee KH, Strand RK. SOFC cogeneration system for building applications, part 1: development of SOFC system-level model and the parametric study. Renew Energ 2009;34: 2831e8.
[12] Qi Y, Huang B, Luo J. Dynamic modeling of a finite volume of solid oxide fuel cell: the effect of transport dynamics. Chem Eng Sci 2006;61:6057e76.
[13] Sunden B, Faghri M. Transport phenomena in fuel cells, series: developments in heat transfer. 1st ed. Massachusetts: Boston; 2005.
[14] Erning JW, Hauber T, Stimming U, Wippermann K. Catalysis of the electrochemical processes on solid oxide fuel cell cathodes. J Power Sources 1996;61:205e11.
[15] Shi Y, Cai N, Li C. Numerical modeling of an anodesupported SOFC button cell considering anodic surface diffusion. J Power Sources 2007;164:639e48.
[16] Bessler WG. A new computational approach for SOFC impedance from detailed electrochemical reaction-diffusion models. Solid State Ion 2005;176:997e1011.
[17] Pakzad A, Salamati H, Kameli P, Talaei Z. Preparation and investigation of electrical and electrochemical properties of lanthanum-based cathode for solid oxide fuel cell. Int J Hydrogen Energy 2010;35:9398e400.
[18] Tsipis EV, Kharton VV. Electrode materials and reaction mechanisms in solid oxide fuel cells: a brief review-I. Performance determining factors. J Solid State Electrochem 2008;12:1039e60.
[19] Santarelli M, Leone P, Calı` M, Orsello G. Experimental activity on a large SOFC generator. In: Vasquez LO, editor. Fuel cell research trends. Nova Science Publishers Inc; 2007. p. 71e134.
[20] Klein JM, Bultel Y, Pons M, Ozil P. Current and voltage distributions in a tubular solid oxide fuel cell (SOFC). J Appl Electrochem 2008;38:497e505.
[21] Oussar Y, Dreyfus G. How to be a gray box model. Neural Networks 2001;14:1161e72.
[22] Abdul-Wahab SA, Bakheit CS, Al-Alawi SM. Principal component and multiple regression analysis in modeling of ground-level ozone and factors affecting its concentrations. Environ Model Softw 2005;20:1263e71.
[23] King JR, Jackson DA. Variable selection in large environmental data sets using principal components analysis. Envirometrics 1999;10:67e77.
[24] Zhao Y, Ou C, Chen J. A new analytical approach to model and evaluate the performance of a class of irreversible fuel cells. Int J Hydrogen Energy 2008;33:4161e70.
[25] Khalheim OM. Scaling of analytical data. Anal Chim Acta 1985;177:71e9.